Inorg. Chem. **2004**, *43*, 8130–8142

Solution Structure and Thermolysis of *Coβ*-5′-Deoxyadenosylimidazolylcobamide, a Coenzyme B_{12} Analogue with an Imidazole Axial Nucleoside

Kenneth L. Brown,*,† Xiang Zou,† Rakesh R. Banka,† Christopher B. Perry,‡ and Helder M. Marques‡

Department of Chemistry and Biochemistry, Ohio University, Athens, Ohio 45701, and Molecular Sciences Institute, School of Chemistry, University of the Witwatersrand, PO Wits, Johannesburg, 2050 South Africa

Received June 11, 2004

The solution structure of *Coβ*-5′-deoxyadenosylimidazolylcobamide, Ado(Im)Cbl, the coenzyme B_{12} analogue in which the axial 5,6-dimethylbenzimidazole (Bzm) ligand is replaced by imidazole, has been determined by NMR-restrained molecular modeling. A two-state model, in which a conformation with the adenosyl moiety over the southern quadrant of the corrin and a conformation with the adenosyl ligand over the eastern quadrant of the corrin are both populated at room temperature, was required by the nOe data. A rotation profile and molecular dynamics simulations suggest that the eastern conformation is the more stable, in contrast to AdoCbl itself in which the southern conformation is preferred. Consensus structures of the two conformers show that the axial Co–N bond is slightly shorter and the corrin ring is less folded in Ado(Im)Cbl than in AdoCbl. A study of the thermolysis of Ado(Im)Cbl in aqueous solution (50–125 °C) revealed competing homolytic and heterolytic pathways as for AdoCbl but with heterolysis being 9-fold faster and homolysis being 3-fold slower at 100 °C than for AdoCbl. Determination of the pK_a's for the Ado(Im)Cbl base-on/base-off reaction and for the detached imidazole ribonucleoside as a function of temperature permitted correction of the homolysis and heterolysis rate constants for the temperature-dependent presence of the base-off species of Ado(Im)Cbl. Activation analysis of the resulting rate constants for the base-on species show that the entropy of activation for Ado(Im)Cbl homolysis (13.7 ± 0.9 cal mol^{-1} K^{-1}) is identical with that of AdoCbl (13.5 ± 0.7 cal mol^{-1} K^{-1}) but that the enthalpy of activation (34.8 kcal mol^{-1}) is 1.0 ± 0.4 kcal mol^{-1} larger. The opposite effect is seen for heterolysis, where the enthalpies of activation are identical but the entropy of activation is 5 ± 1 cal mol^{-1} K^{-1} less negative for Ado(Im)Cbl. Extrapolation to 37 °C provides a rate constant for Ado(Im)Cbl homolysis of 2.1×10^{-9} s^{-1}, 4.3-fold smaller than for AdoCbl. Combined with earlier results for the enzyme-induced homolysis of Ado(Im)Cbl by the ribonucleoside triphosphate reductase from *Lactobacillus leichmannii*, the catalytic efficiency of the enzyme for homolysis of Ado(Im)Cbl at 37 °C can be calculated to be 4.0×10^8, 3.8-fold, or 0.8 kcal mol^{-1}, smaller than for AdoCbl. Thus, the bulky Bzm ligand makes at best a <1 kcal mol^{-1} contribution to the enzymatic activation of coenzyme B_{12}.

Introduction

Coenzyme B_{12}- (5′-deoxyadenosylcobalamin, AdoCbl, Figure 1) dependent enzymes are remarkable in their ability to catalyze the homolysis of the carbon−cobalt bond of the coenzyme by some 10^9−10^{14}-fold (13−18 kcal mol^{-1}),[1−4] the so-called "activation" of AdoCbl, an enormous acceleration for the simple dissociation of a single bond. There has long been interest in the question of whether the axial nucleotide plays a significant role in the activation of the coenzyme, and this interest has only been heightened by recent findings that different AdoCbl-dependent enzymes manipulate the axial ligation of the coenzyme in different ways. Thus, the class I and class III enzymes,[5] the mutases

* Author to whom correspondence should be addressed. E-mail: brownk3@ohiou.edu.
† Ohio University.
‡ University of the Witwatersrand.

(1) Brown, K. L.; Li, J. *J. Am. Chem. Soc.* **1998**, *37*, 9466.
(2) Brown, K. L.; Zou, X. *J. Inorg. Biochem.* **1999**, *77*, 185.
(3) Chowdhury, S.; Banerjee, R. *Biochemistry* **2000**, *39*, 7998.
(4) Toraya, T. *Chem. Rec.* **2002**, *2*, 352.

10.1021/ic040079z CCC: $27.50
Published on Web 11/06/2004

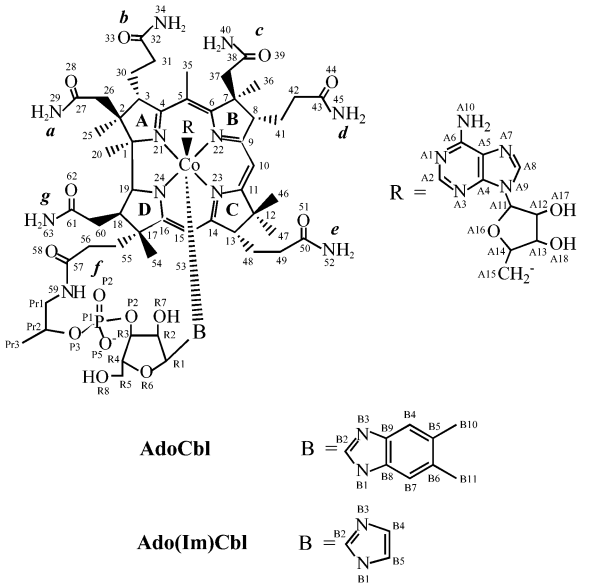

Figure 1. Structure and numbering scheme for AdoCbl and Ado(Im)Cbl.

and aminomutases, respectively, bind AdoCbl by displacing the axial 5,6-dimethylbenzimidazole (Bzm) nucleotide with an imidazole moiety from an active site His residue while burying the nucleotide loop in a hydrophobic pocket,[6,7] the so-called "base-off/His-on" binding mode, while the class II enzymes, the eliminases and AdoCbl-dependent ribonucleotide reductases, bind the coenzyme in the base-on mode, with the Bzm nucleotide coordinated to the metal.[8,9]

Perhaps the most well studied of the proposed mechanisms for enzymatic activation of AdoCbl involving the axial nucleotide are the so-called "mechanochemical triggering" mechanisms.[10] The classical version of mechanochemical triggering envisions ground-state destabilization of AdoCbl by enzymatic compression of the long (2.24 Å)[11] axial Co−N bond leading to a sterically induced increase in the upward fold of the corrin ring,[12] and consequent steric pressure on the axial Co−C bond stretching and weakening it. While such steric compression of the axial Co−N bond would require a considerable amount of energy, it is now clear that proteins are capable of binding Cbl's enormously tightly[1,2,13] while binding constants for AdoCbl to AdoCbl-dependent enzymes are many orders of magnitude smaller, suggesting that ample amounts of binding energy may well be available for such bond compression.

Theoretical studies of ground-state mechanochemical triggering[14] have confirmed the feasibility of this mechanism. Thus, when the axial Co−N bond of AdoCbl is compressed in molecular mechanics simulations, the corrin ring fold angle is increased, the Co−C bond is stretched, and the Co−C−C bond angle is increased. The effect is clearly a steric one, since when the axial Bzm ligand is replaced by imidazole (*Coβ*-5′-deoxyadenosylimidazolylcobamide, Ado(Im)Cbl, Figure 1), all three geometrical effects are reduced. Overall, however, the effects of such mechanochemical triggering on the Co−C bond were small and deemed unlikely to contribute more than a few kcal mol^{-1} to the enzymatic activation of AdoCbl.[14]

We also considered an alternate version of this mechanism, dubbed "transition state mechanochemical triggering", in which the possibility of electronic stabilization of the transition state for Co−C bond homolysis via Co−N_{ax} bond compression leads to improved Co−N orbital overlap. However, it is now clear that Co−C bond homolysis at an enzyme active site is a simple bond dissociation reaction, so that the reaction coordinate diagram has no maximum and there is no transition state.[15] Consequently, catalysis can only be affected by destabilization of the reactant or stabilization of the product, cob(II)alamin. The situation is different for thermally induced homolysis in solution. Here, the immediate products of Co−C bond dissociation are a caged radical pair, the separation of which must traverse a diffusion transition state to form the free radical products. Thus, activation energies for thermal homolysis in solution contain both the energetics of bond dissociation and the activation energy for diffusion.

(5) (a) Bückel, W.; Golding, B. T. *Chem. Soc. Rev.* **1996**, 329. (b) Golding, B. T.; Bückel, W. In *Comprehensive Biochemical Catalysis*; Sinnott, M. L., Ed.; Academic Press: London, 1997; Vol. 3, pp 239−259.

(6) (a) Padmakumar, R.; Taoke, S.; Padmakumar, R.; Banerjee, R. *J. Am. Chem. Soc*. **1995**, *117*, 7033. (b) Zelder, O.; Beatrix, B.; Kroll, F.; Bückel, W. F*EBS Lett.* **1995**, *369*, 252. (c) Mancia, F.; Keep, N. H.; Nakagawa, A.; Leadley, P. F.; McSweeney, S.; Rasmussen, B.; Bösecke, P.; Diat, O.; Evans, P. R. *Structure (London)* **1996**, *4*, 339. (d) Thomä, N. H.; Meier, T. W.; Evans, P. R.; Leadley, P. F. *Biochemistry* **1998**, *37*, 14386. (e) Mancia, F.; Evans, P. R. *Structure (London*) **1998**, *6*, 711. (f) Reitzer, R.; Gruber, K.; Jogl, G.; Wagner, U. G.; Bothe, H.; Bückel, W.; Kratky, C. *Structure (London)* **1999**, *7*, 891.

(7) (a) Chang, C. H.; Frey, P. A. *J. Biol. Chem*. **2000**, *275*, 106. (b) Chen, H.-P.; Wu, S.-H.; Lin, Y.-L.; Chen, C.-M.; Tsay, S.-S. *J. Biol. Chem*. **2001**, *276*, 44744.

(8) (a) Yamanishi, M.; Yamada, S.; Muguruma, H.; Murakami, Y.; Tobimatsu, T.; Ishida, A.; Yamauchi, J.; Toraya, T. *Biochemistry* **1998**, *37*, 4799. (b) Abend, A.; Nitsche, R.; Bandarian, V.; Stupperich, E.; Rétey, J. *Angew. Chem., Int. Ed*. **1998**, *37*, 625. (c) Abend, A.; Bandarian, V.; Nitsche, R.; Stupperich, E.; Rétey, J.; Reed, G. H. *Arch. Biochem. Biophys.* **1999**, *370*, 138. (d) Ke, S. C.; Torrent, M.; Museav, D. G.; Morokuma, K.; Warncke, K. *Biochemistry* **1999**, *38*, 12681. (e) Shibata, N.; Masuda, J.; Tobimatsu, T.; Toraya, T.; Suto, K.; Morimoto, Y.; Yasuoka, N. *Structure (London)* **1999**, *7*, 997. (f) Masude, J.; Shibata, N.; Morimoto, Y.; Toraya, T.; Yasuoka, N. *Structure (London)* **2000**, *8*, 775. (g) Bandarian, V. P.; Reed, G. H. *Biochemistry* **2002**, *41*, 8580.

(9) (a) Lawrence, C. C.; Gerfen, G. J.; Samano, V.; Nitsche, R.; Robins, M. J.; Rétey, J.; Stubbe, J. *J. Biol. Chem.* **1999**, *274*, 7039. (b) Sintchak, M. D.; Arjara, G.; Kellogg, B. A.; Stubbe, J.; Drennan, C. L. *Nat. Struct. Biol*. **2002**, *9*, 293.

(10) (a) Grate, J. H.; Schrauzer, G. N. *J. Am. Chem. Soc.* **1979**, *101*, 4601. (b) Schrauzer, G. N.; Grate, J. H. *J. Am. Chem. Soc*. **1981**, *103*, 541. (c) Bresciani-Pahor, N.; Forcolin, M.; Marzilli, L. G.; Randaccio, L.; Summers, M. F.; Toscano, P. J. *Coord. Chem. Rev*. **1985**, *63*, 1. (d) Toraya, T.; Ishida, A. *Biochemistry* **1988**, *27*, 7677. (e) Marques, H. M.; Brown, K. L.; Jacobsen, D. W. *J. Biol. Chem.* **1988**, *263*, 12378. (f) Brown, K. L.; Brooks, H. B. *Inorg. Chem*. **1991**, *30*, 3420. (g) Summers, M. F.; Toscana, P. J.; Bresciani-Pahor, N.; Nardin, G.; Randaccio, L.; Marzilli, L. G. *J. Am. Chem. Soc*. **1983**, *105*, 6259.

(11) Savage, H. F. J.; Lindley, P. F.; Finney, J. L.; Timmins, P. A. *Acta Crystallogr*. **1987**, *B43*, 280.

(12) (a) The corrin ring fold angle is defined[12b] as the angle between the normals to the least-squares planes through N21, C4, C5, C6, N22, C9, and C10 and through N24, C16, C15, C14, N23, C11, and C10. (b) Glusker, J. P. In B_{12}; Dolphin, D., Ed.; Wiley: New York, 1982; Vol. 1, pp 23−106.

(13) Marchaj, A.; Jacobsen, D. W.; Savon, S. R.; Brown, K. L. *J. Am. Chem. Soc*. **1995**, *117*, 11640.

(14) (a) Sirovatka, J. M.; Rappé, J. M.; Finke, R. G. *Inorg. Chim. Acta* **2000**, *300*, 545. (b) Brown, K. L.; Marques, H. M. *J. Inorg. Biochem*. **2001**, *83*, 121.

(15) Brown, K. L.; Marques, H. M. *J. Inorg. Biochem*., submitted for publication.

Scheme 1

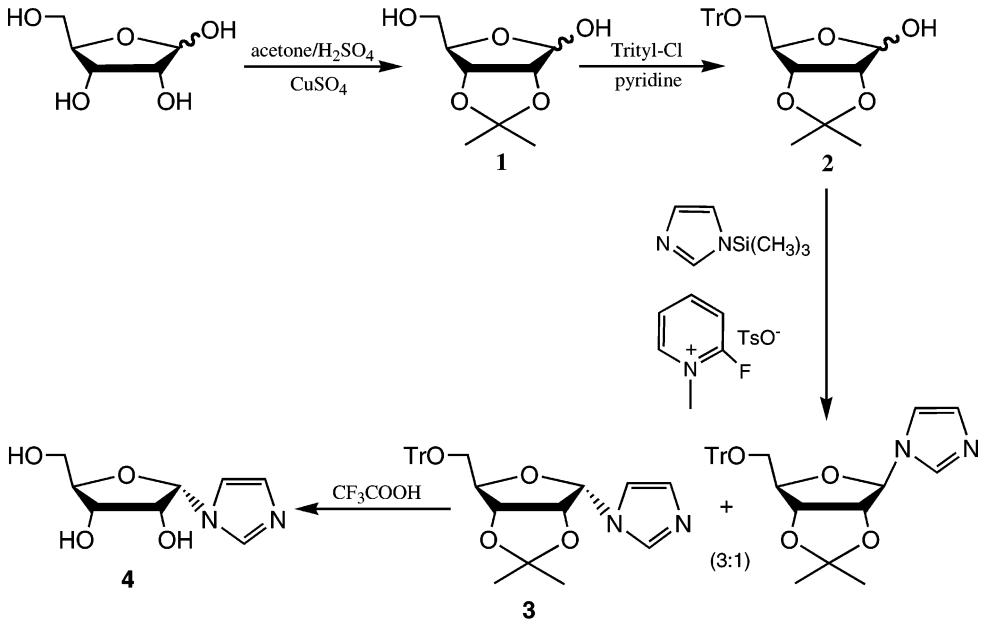

The kinetics for the enzyme-induced Co−C bond homolysis of Ado(Im)Cbl by the AdoCbl-dependent ribonucleoside triphosphate reductase(RTPR) from *Lactobacillus leichmannii* have already been reported.[16] At 37 °C, Ado(Im)Cbl was found to undergo RTPR-induced Co−C bond homolysis 16.5-fold more slowly than AdoCbl itself.[1,17] However, the catalytic efficiency of the enzyme for Ado(Im)Cbl activation is unknown, as the nonenzymatic, thermal homolysis of Ado(Im)Cbl has not yet been reported. In *Coβ*-cyanoimidazolylcobamide (CN(Im)Cbl) and *Coβ*-methylimidazolylcobamide (CH_3(Im)Cbl), the imidazole-substituted analogues of cyanocobalamin (CNCbl) and methylcobalamin (CH_3Cbl), the corrin ring fold angles are reduced from 18.0° (in CNCbl) to 11.3° and from 14.7° (in CH_3Cbl) to 12.2°.[18] As shown by the molecular mechanics studies[14] of mechanochemical triggering, a similar reduction in the corrin ring fold angle of Ado(Im)Cbl would be expected to decrease its lability toward thermal homolysis. We now report a complete kinetic and product study of the thermolysis of Ado(Im)Cbl, including deconvolution of the anticipated homolytic and heterolytic thermolysis pathways and correction for the significant occurrence of base-off species. The results allow the calculation of the rate constant for thermal homolysis of the base-on species at 37 °C and hence calculation of the catalytic efficiency of RTPR for activation of Ado(Im)Cbl.

Experimental Section

CN(Im)Cbl was obtained by "guided biosynthesis",[18,19] i.e., fermentation of *Propionibacterium shermanii* on media supplemented with imidazole, and converted to Ado(Im)Cbl as previously described.[16] [2-^{3}H]5′-chloro-5′-deoxyadenosine was obtained as described previoulsy[2] and was used to alkylate CN(Im)Cbl to form [A2-^{3}H]Ado(Im)Cbl, analogous to the previously reported synthesis of [A2-^{3}H]AdoCbl.[2] Organic chemicals and solvents were obtained from Aldrich or Fisher Scientific in the highest purity available and used without further purification.

Synthesis of 1-α-D-Ribofuranosylimidazole (4). The synthesis of the axial ribonucleoside of Ado(Im)Cbl was achieved as shown in Scheme 1.

2,3-Isopropylidene-D-ribofuranose (1).[20] Dry D-ribose (2.0 g, 13.3 mmol) was suspended in 40 mL (0.54 mol) of dry acetone (distilled over type 4A molecular sieves) and 0.1 mL concentrated H_2SO_4. Anhydrous copper sulfate (4.0 g, dried at 250 °C for 2 h) was added, and the mixture was stirred for 20 h. The copper sulfate was filtered out and washed with acetone (3 × 5 mL). The filtrate and combined washings were neutralized by stirring with calcium hydroxide for 1 h. The calcium sulfate and excess calcium hydroxide were removed by filtration and the solids washed with acetone (3 × 5 mL). The combined filtrate and washings were evaporated to dryness under reduced pressure at 30 °C to yield 2.1 g (84%) of **1**. ^{1}H NMR ($CDCl_3$): δ 5.41 (1H, d, 1′), 4.82 (1H, d, 2′), 4.57 (1H, t, 3′), 4.38 (1H, m, 4′), 3.76 (2H, m, 5′), 1.49 (3H, s, Me), 1.33 (3H, s, Me).

2,3-Isopropylidene-5-trityl-D-ribofuranose (2).[21] 2,3-Isopropylidene-D-ribofuranose (**1**), 2.1 g (11.1 mmol), was dissolved in 10 mL of dry pyridine and treated with 3.3 g (11.8 mmol) of dry trityl chloride (dried over P_2O_5). After the mixture was stirred for about 10 h, some precipitate had formed, but the reaction was allowed to proceed for 24 h. The mixture was poured into water (50 mL), the aqueous supernatant was decanted, and the remaining precipitate was washed with water and dissolved in CH_2Cl_2 (30 mL). The solution was shaken with 4 g of cadmium chloride in 40 mL of water, and the white solid which formed was filtered off. The aqueous and organic layers were separated, and the CH_2Cl_2 layer was washed with water and dried over Na_2SO_4. Evaporation of the solvent yielded a syrup (4.7 g). The product was purified

(16) Brown, K. L.; Zou, X.; Li, J.; Chen, G. *Inorg. Chem.* **2001**, *40*, 5942.
(17) Licht, S. S.; Lawrence, C. C.; Stubbe, J. *Biochemistry* **1999**, *38*, 1234.
(18) (a) Kräutler, B.; Konrat, R.; Stupperich, E.; Färber, G.; Gruber, K.; Kratky, C. *Inorg. Chem.* **1994**, *33*, 4128. (b) Fasching, M.; Schmidt, W.; Kräutler, B.; Stupperich, E.; Schmidt, A.; Kratky, C. *Helv. Chim. Acta* **2000**, *83*, 2295. (c) Randaccio, L.; Furlan, M.; Geremia, S.; Slouf, M.; Srnova, I.; Toffoli, D. *Inorg. Chem.* **2000**, *39*, 3403.
(19) (a) Renz, P. *Methods Enzymol.* **1971**, *18C*, 82. (b) Hörig, J. A.; Renz, P.; Heckmann, G. *J. Biol. Chem.* **1978**, *253*, 7410. (c) Stupperich, E.; Steiner, I.; Rühlemann, M. *Anal. Biochem.* **1986**, *155*, 365.
(20) Levene, P. A.; Stiller, E. T. *J. Biol. Chem.* **1933**, *102*, 187.
(21) Klein, R. S.; Ohrui, H.; Fox, J. J. *J. Carbohydr. Nucleosides Nucleotides* **1974**, *1*, 265.

by column chromatography on silica gel, eluting with a gradient of 5−10% ethyl acetate in hexanes. ^{1}H NMR showed it to be a mixture of α and *β* anomers of the protected ribose. Yield: 2.0 g (42%).

2,3-Isopropylidene-5-trityl-α-D-ribofuranosylimidazole (3).[22] A solution of 2,3-isopropylidene-5-trityl-D-ribofuranose, **2** (149 mg, 0.345 mmol), and *N*-ethyldiisopropylamine (98 mg, 0.76 mmol) in 3 mL of CH_2Cl_2 was added to a stirred suspension of 2-fluoro-1-methylpyridinium *p*-toluenesulfonate (160 mg, 0.57 mmol) in 1.5 mL of CH_2Cl_2 at −30 °C. The suspension was stirred for 3 h while the temperature was slowly raised to −5 °C, during which time the colorless suspension gradually turned yellow. To this yellowish suspension was added 1-(trimethylsilyl)imidazole (190 mg, 0.135 mmol) in 3 mL of CH_2Cl_2, and the solution was stirred for 20 h at 4 °C and then for 20 h at room temperature. The solvent was removed by evaporation, and the product was purified by chromatography on silica gel, eluting with chloroform. The yield was 120 mg (73%). The ^{1}H NMR spectrum revealed a mixture of α and *β* anomers in a ratio of about 3:1. The anomers were separated on silica gel using a gradient elution of 10−25% ether in benzene. *β*-Anomer: ^{1}H NMR ($CDCl_3$) *δ* 7.67 (1H, s, Im), 7.23−7.41 (15H, m, Tr), 7.05 (1H, s, Im), 7.03 (1H, s, Im), 5.76 (1H, d, 1′), 4.79 (1H, m, 2′), 4.74 (1H, m,3′). 4.38 (1H. q. 4′), 3.31 (2H, m, 5′), 1.58 (3H, s, CH_3), 1.35 (3H, s, CH_3); ^{13}C NMR ($CDCl_3$) *δ* 143.25 (Ph_3C, 135.69 (Im), 130.48 (Im), 128.64−127.23 (Tri), 116.24 (Im), 114.69 (^{i}Pr), 91.92 (1′), 87.10 (^{i}Pr), 85.31 (3′), 84.45 (4′), 81.27 (2′), 63.52 (5′), 27.23 (CH_3), 25.38 (CH_3). α-Anomer: ^{1}H NMR ($CDCl_3$) *δ* 7.73 (1H, s, Im), 7.27−7.39 (15H, m, Tr), 7.13 (1H, s, Im), 7.09 (1H, s, Im), 6.21(1H, d, 1′), 4.92 (1H, q, 2′), 4.78 (1H, d, 3′), 4.39 (1H, t, 4′), 3.38 (2H, dq, 5′), 1.45 (3H, s, CH_3), 1.31 (3H, s, CH_3); ^{13}C NMR ($CDCl_3$) *δ* 143.35 (Ph_3C), 136.68 (Im), 128.50 (Im), 128.45−127.40 (Tri), 118.33 (Im), 113.71 (^{i}Pr), 88.62 (1′), 87.75 (^{i}Pr), 82.48 (3′), 82.09 (4′), 80.58 (2′), 65.36 (5′), 25.78 (CH_3), 24.49 (CH_3).

1-α-D-Ribofuranosylimidazole (4).[23] 2,3-Isopropylidene-5-trityl-α-D-ribofuranosylimidazole (**3**) (0.2 g, 0.42 mmol) was dissolved in trifluoroacetic acid (3 mL), and the solution was stirred for 3 h. The solution was evaporated to dryness under reduced pressure, and the residual oil was pumped under high vacuum for 1 h. The solid residue was mixed with water (25 mL) and chloroform (25 mL) and the water layer was separated, washed twice with chloroform, and evaporated to give the product in 96% yield (80 mg). ^{1}H NMR (D_2O): *δ* 8.89 (1H, s, Im), 7.63 (1H, s, Im), 7.49 (1H, s, Im), 6.24 (1H, d, 1′), 4.64 (1H, t, 2′), 4.48 (1H, m, 3′), 4.34 (1H, m, 4′), 3.79, (2H, dq, 5′). ^{13}C NMR (D_2O): *δ* 136.58 (I2), 123.58 (I4), 121.75 (I5), 91.55 (R1′), 88.81 (R2′), 74.21 (R4′), 72.90 (R3′), 63.73 (R5′).

Spectroscopic Methods. UV−visible spectroscopic measurements were made on a Cary 3 spectrophotometer, the sample compartment of which was thermostated at the appropriate temperature. One- and two-dimensional NMR spectra were obtained on a Varian Unity Inova 500 MHz NMR spectrometer.

Molecular Modeling. All molecular mechanics calculations were performed using the MM+ force field, a version of Allinger's MM2(87) program,[24] included in the HYPERCHEM suite of programs (version 7.03),[25] but using parameters developed specifically for modeling the cobalt corrinoids.[26] Geometry optimizations were performed using a conjugate-gradient algorithm when the structure was far from the energy minimum and then the faster Newton−Raphson block-diagonal method. Energy minimization was terminated when an rmsd of 0.05 kcal mol^{-1} Å^{-1} in the gradient was attained. The crystal structure of AdoCbl,[11] with the appropriate atoms in the Bzm base removed, was used as the starting point for modeling Ado(Im)Cbl. Molecular dynamics/simulated annealing (MD/SA) calculations were performed by integrating Newton's equations of motion using the leapfrog algorithm[27] with a time step of 1 fs. The temperature was controlled by coupling the system to a simulated heat bath[28] with a bath relaxation time of 0.1 ps. All atoms in the starting structure were assigned random initial velocities before MD or MD/SA calculations were performed.

MD simulations used an initial heating phase of 5 ps from 0 K to the desired run temperature and a run phase that varied between 0 and 24 ps at 600 K for simulations designed to discover stable conformations (or performed at 300 K for 300 ps in simulations used for exploring interproton distances at room temperature), and the run phase was followed by a cooling phase from the run temperature to 0 K over 10 ps, followed by full energy minimization.

nOe restraints were applied as described earlier.[29] All prochiral protons were assigned on a trial and error basis until the minimum number of distance criteria violations were observed during a 100 ps simulation at 300 K. In cases where a number of nOe's to the same achiral center were observed, the proton pair with the smallest inter-proton distance was chosen for each restraint.

Steric barriers to rotation of the Ado ligand in Ado(Im)Cbl were examined by driving the N24−Co−A15−A14 torsional angle, ω_1, through 360° in 5° increments, rotating the ligand in both a clockwise and counterclockwise direction. At each 5° interval of ω_1, a full energy minimization was performed, and the structure with the lowest strain energy at each value of ω_1 was accepted. All negative torsion angles measured (−180 to 0°) were normalized to positive values (0 to 360°), except in cases where a distribution lay on either side of 0°.

Ado(Im)Cbl Thermolysis Kinetics. All reactions involving Ado(Im)Cbl were carried out in the dark. The progress of anaerobic thermolysis of Ado(Im)Cbl was monitored by two different methods. In the spectrophotometric method,[30] a solution of Ado(Im)Cbl (0.4 mM) in 0.1 M aqueous potassium phosphate buffer (pH 7.0) with 20 mM 4-hydroxy-2,2,6,6-tetramethylpiperidinyloxy (H-TEMPO) at ionic strength 1.0 M (KCl) was placed in a 1 mL quartz cuvette equipped with a high-vacuum Schlenk valve and deoxygenated by passing water-saturated argon through the cuvette for at least 4 h before sealing. The spectrum of the solution was recorded from 850 to 400 nm, the cuvette was then heated at the appropriate temperature (90−125 °C) for a predetermined length of time, and the spectrum was recorded again after rapid cooling to room temperature. Kinetic data at 650 nm were extracted from the scans and used to determine the rate constant as described elsewhere.[30] A radiometric method, using [A2-^{3}H]Ado(Im)Cbl, was

(22) Mukaiyama, T.; Hashimoto, Y.; Hayashi, Y.; Shoda, S.-I. *Chem. Lett.* **1984**, 557.
(23) DeBarnardo, S.; Weigele, M. *J. Org. Chem.* **1976**, *41*, 287.
(24) (a) Allinger, N. L.; Yun, Y. *MM2(87)*; distributed to academic users by QCPE, under special agreement with Molecular Design Ltd., San Leandro, CA. (b) Allinger, N. L. *J. Am. Chem. Soc.* **1979**, *99*, 8127.
(25) *HYPERCHEM*; Hypercube Ltd., 1115 NW Street, Gainesville, FL, 32601.
(26) (a) Marques, H. M.; Brown, K. L. *J. Mol. Struct. (THEOCHEM)* **1995**, *340*, 97. (b) Marques, H. M.; Warden, C.; Monye, M.; Shongwe, M. S.; Brown, K. L. *Inorg. Chem.* **1998**, *37*, 2578.
(27) Hockney, R. W. *Methods Comput. Phys.* **1970**, *9*, 136.
(28) Berendsen, H. J. C.; Postma, J. P. M.; van Gunsteren, W. F.; DiNola, A.; Haak, J. R. *J. Chem. Phys.* **1984**, *81*, 3684.
(29) (a) Brown, K. L.; Zou, X.; Marques, H. M. *J. Mol. Struct. (THEOCHEM)* **1998**, *453*, 209. (b) Brown, K. L.; Cheng, S.; Zou, X.; Li, J.; Chen, G.; Valente, E. J.; Zubkowski, J. D.; Marques, H. M. *Biochemistry* **1998**, *37*, 9704.
(30) Brown, K. L.; Zou, X.; Chen, G.; Xia, Z.; Marques, H. M. *J. Inorg. Biochem.* **2004**, *98*, 287.

used to determine the rate constant for Ado(Im)Cbl thermolysis at 105, 70, and 50 °C (using the method of initial rate for the two lower temperatures) as described previously.[2]

Product Analysis. Product analysis was conducted by reverse phase HPLC as previously described for AdoCbl thermolysis.[2] We have previously shown that all nucleoside derived products from the adenosyl group of AdoCbl are stable at elevated temperatures.[2] Under these reaction conditions for Ado(Im)Cbl thermolysis, only two nucleoside derived products, adenine and 5′-deoxy-5′-(4-hydroxy-2,2,6,6-tetramethylpiperidinyloxy)adenosine (Ado-H-TEMPO), were observed at all temperatures (70−125 °C). The ratio of these products was determined from peak integration of the HPLC chromatograms after correction for the difference in molar absorbtivity in the temperature range 10−49 °C as reported previously.[30,31] For the detached nucleoside, 1-α-D-ribofuranosylimidazole (**4**), the pK_a for its conjugate acid was determined potentiometrically.

Acid−Base Chemistry of Ado(Im)Cbl. Values for the apparent pK_a for the base-on/base-off equilibrium of Ado(Im)Cbl (p$K_{base-off}$, eq 1) were determined spectrophotometrically by titration with 0.1 M NaOH (ionic strength 1.0 M, KCl) under an argon atmosphere at temperatures from ca. 10 to 50 °C.

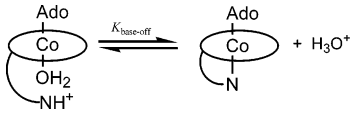

(1)

Results

Solution Structure of Ado(Im)Cbl. Since Ado(Im)Cbl refused to crystallize, preventing the determination of an X-ray crystal structure, a solution structure was determined using NMR-restrained molecular modeling. A preliminary 100 ps MD simulation of Ado(Im)Cbl at 300 K resulted in 5 observed nOe's that had mean H−H distances that violated the distance criteria. This prompted an investigation of the energy consequence of rotating the Ado ligand about the Co−A15 bond by a full 360° relative to the corrin ring with all Ado to non-Ado restraints released. Four energy minima were found in the rotation profile (Figure 2), corresponding to the "southern" conformation ($\omega_1 \approx 35°$) observed in the crystal structure of AdoCbl itself,[11] a "northeastern" conformation ($\omega_1 \approx 140°$), and two "western" conformations ($\omega_1 \approx 235°$, $\omega_1 \approx 275°$), with the northeastern conformation being the global minimum. A 300 ps MD simulation performed while monitoring the N24−Co−A15−A14 torsion, with all Ado to non-Ado restraints excluded, showed that the Ado ligand spends the majority of its time in the northeastern conformation, with the southern and western conformations rarely visited (Figure 2). All but two (Table S1, Supporting Information; N63, A11−C26, and N88, A8−A11) of the violating nOe's could be accounted for by adopting a "two-state" approach in which the modeling was performed with either the nOe's that are compatible only with the northeastern conformation removed (Table S1; N6, C46−A14, and N61, A11−C46) or those compatible only with the southern conformation removed (Table S1; N21, C54−A14, N62, A11−C54, and N63, A11−C26). The former is referred to as modeling the southern conformation,

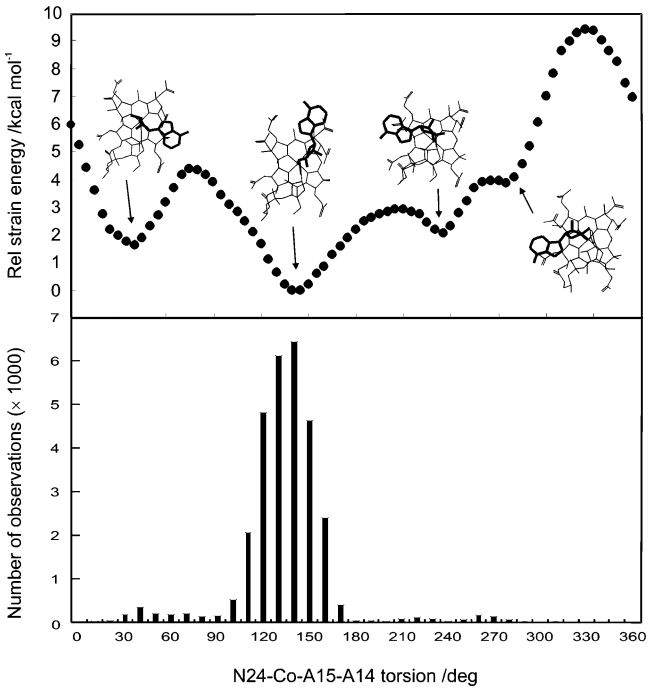

Figure 2. Strain energy profile and probability distribution for rotation of the Ado ligand of Ado(Im)Cbl about the Co−C bond as a function of the torsion angle, ω_1, N24−Co−A15−A14.

and the latter as modeling the "eastern" conformation.[32] The A11−C26 violation could be accounted for by a western conformation, but when such a conformation was modeled, the Ado consistently adopted orientations ranging from the southern to the eastern conformation.

A 300 ps MD simulation of the southern conformation reveals that the Ado ligand visits a fairly wide range of orientations in relation to the corrin ring. The range of values for the N24−Co−A15−A14 torsion was −105.8 to 61.2° (mean 29.3° ± 10°), so that that the Ado moiety moves within an arc from where Ade is directly above the C1−C19 bridge to where it is above C46 but is largely confined to a position above the C ring. The Ado group visits a narrower range of angles in the eastern conformation, but there is more freedom of movement as indicated by the larger standard deviation; the N24−Co−A15−A14 torsion ranged from 33.3 to 149.5° (mean 111.4° ± 17°). In the eastern conformation, the arc of movement of the Ado moiety begins where the ligand is in the southern conformation and extends to where Ade is roughly positioned over the B ring.

Movement of the Ade with respect to the ribose was investigated by monitoring the A8−A9−A11−A12 torsion. In both the southern and eastern conformations, the Ade moiety remains virtually parallel to the corrin ring, with the range of values for this torsion in the southern conformation being −141.1 to −1.5° (mean −51.7° ± 13.7°) and for the eastern conformation −110.3 to 43.8° (mean −51.1° ± 15.9°). Despite this considerable freedom of motion in both conformations, Ade remains in the anti conformation relative

(31) Brown, K. L.; Hakimi, J. M.; Nuss, D. M.; Mantejano, Y. D.; Jacobsen, D. W. *Inorg. Chem.* **1984**, *23*, 1463.

(32) (a) Brown, K. L.; Marques, H. M. *Polyhedron* **1996**, *15*, 2187. (b) Brown, K. L.; Marques, H. M. *J. Mol. Struct.* **2000**, *520*, 75. (c) With the Ado to non-Ado restraints enforced, the northeastern conformation becomes more eastern (vide infra).

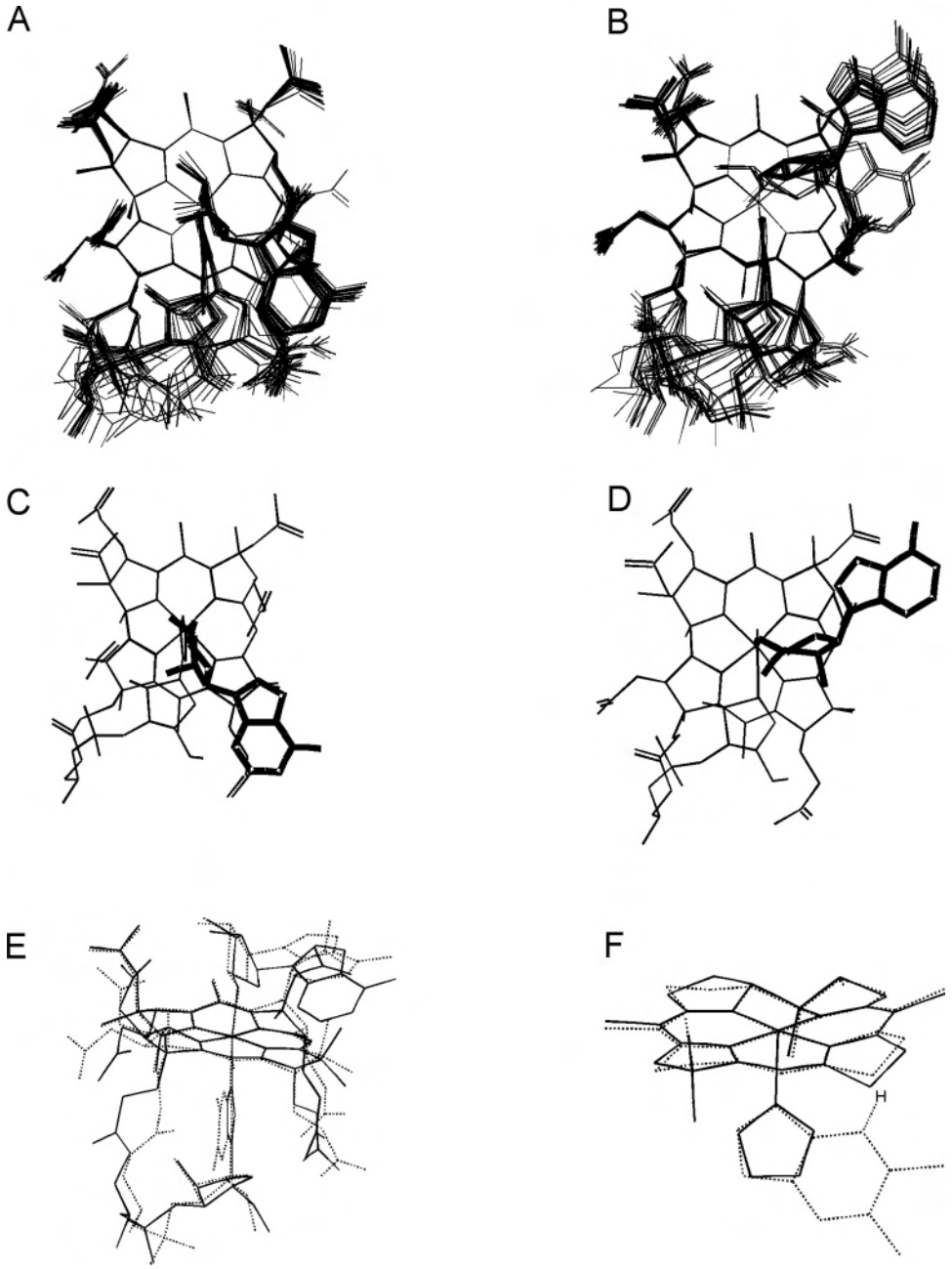

Figure 3. Superposition of 25 annealed structures of the (A) southern and (B) eastern conformations of Ado(Im)Cbl, consensus structures for the (C) southern and (D) eastern conformations generated by averaging the coordinates for the 25 annealed structures, (E) an overlay of the consensus structure of the southern conformation with the crystal structure of AdoCbl, and (F) an overlay of the corrin ring and axial base for the consensus structure of the Ado(Im)Cbl southern conformation and the crystal structure of AdoCbl, viewed along the C10−Co direction.

to the ribose, and no evidence was found during the 300 ps simulation for the syn conformation. One of the observed nOe's that gave a mean H−H distance violation (Table S1; N88, A8−A1) does however suggest that the syn conformation is visited in solution. However, simulations in which the Ade moiety was originally placed in the syn conformation invariably led to reversion to the anti conformation within the first few picoseconds.

A total of 25 solution structures each for the southern and eastern conformations of Ado(Im)Cbl were generated by MD/SA calculations, and the superpositions of these structures are shown in Figure 3 A,B. Annealed structures obtained by modeling the southern conformation indicate that the Ado ligand is confined to a narrow range of orientations relative to the corrin ring but the variation of the Ado ligand position is somewhat greater in the eastern conformation. While the majority of the structures annealed with the Ado ligand in the eastern conformation, but four structures annealed with the Ado ligand in a southeastern orientation.

The ribose ring and nucleotide loop annealed into a wide range of orientations in both the southern and eastern conformations, indicating a large amount of flexibility in this portion of the molecule (Figure 3A,B). Previous modeling of cobalamin compounds[29,32b,33] has shown that orientations of the nucleotide loop range from an "inward" conformation (where O58 points southeast) to an "outward" conformation

Table 1. Comparison of the Coordination Sphere and Corrin Ring Fold Angle in the Molecular Modeling Structures of AdoCbl and Ado(Im)Cbl and the Crystal Structure of AdoCbl

compd	param	annealed structures max	annealed structures min	annealed structures mean (sd)	consensus structure	cryst structure
		Coordination Sphere				
AdoCbl[a]						
southern conf	Co−A15 (Å)	2.053	2.029	2.046(5)	2.046	2.05,[b] 2.04,[c] 2.00,[c] 1.98,[c] 2.023[d]
	Co−A15−A14 (deg)	125.4	121.2	122.5(1.1)	121.7	125,[b] 121,[c] 124,[c] 124,[c] 122.5[d]
	Co−NB3 (Å)	2.179	2.167	2.177(3)	2.171	2.23,[b] 2.24,[c] 2.22,[c] 2.20[d]
eastern conf	Co−A15 (Å)	2.140	2.028	2.065(34)	2.060	
	Co−A15−A14 (deg)	138.5	121.2	125.8(6.4)	122.2	
	Co−NB3 (Å)	2.189	2.175	2.180(4)	2.179	
Ado(Im)Cbl						
southern conf	Co−A15 (Å)	2.049	2.029	2.038(4)	2.041	
	Co−A15−A14 (deg)	127.0	121.7	122.7(1.2)	122.0	
	Co−NB3 (Å)	2.161	2.151	2.155(3)	2.152	
eastern conf	Co−A15 (Å)	2.055	2.016	2.044(11)	2.050	
	Co−A15−A14 (deg)	123.1	120.9	121.7(0.5)	122.0	
	Co−NB3 (Å)	2.160	2.152	2.157(2)	2.157	
		Corrin Fold Angles (deg)				
AdoCbl[a]						
southern conf		16.9	12.2	13.9(1.5)	13.5	14.8,[b] 12.8,[c] 13.3,[c] 14.1,[c] 13.4[d]
eastern conf		15.4	10.2	12.4(1.9)	11.9	
Ado(Im)Cbl						
southern conf		13.4	8.6	10.7(1.5)	11.8	
eastern conf		15.5	5.8	12.4(2.3)	10.9	

[a] Reference 32a. [b] Reference 35a. [c] Reference 11. [d] Reference 35b.

(where O58 points westward). This represents a significant difference between the calculated and solid-state structures of cobalamins, as the majority of cobalamins crystallize with the nucleotide loop in an inward conformation. One example does exist however with the nucleotide loop in an outward conformation.[34] In Ado(Im)Cbl, the nucleotide loop annealed into the outward conformation the majority of the time, although some inward conformations were also obtained.

The consensus structures for the southern and eastern conformations, obtained by averaging the coordinates of the 25 annealed structures for each conformation, were very similar to each other (Figure 3C,D), except for the orientation of the Ado ligand relative to the corrin ring. A major difference was also observed in the orientation of the g side chain, which is upwardly axial in the southern conformation but equatorial in the eastern conformation.

An overlay of the consensus structure of the southern conformation of Ado(Im)Cbl and the crystal structure of AdoCbl is shown in Figure 3E. Except for differences in the side chain orientations and the lower α ligand, the two structures are similar. Minor differences occur in the B−D corrin rings, which appear to be somewhat flatter in the Ado(Im)Cbl. In the consensus structure of Ado(Im)Cbl, the "tilt angle" of the α ligand (defined as the average of the Co−NB3−CB9 and Co−NB3−CB2 bond angles)[18a] is less than in the crystal structure of AdoCbl (Figure 3F).

Table 1 lists the values for the calculated Co−A15 and Co−NB3 bond lengths and Co−A15−A14 angle obtained from the 25 annealed structures and consensus structures of the southern and eastern conformations of Ado(Im)Cbl, along with the molecular mechanics results for AdoCbl and the AdoCbl crystal structure values. The axial bond lengths and Co−A15−A14 bond angles are very similar for the southern and eastern conformations for both the annealed and consensus structures. The consensus structure Co−A15−A14 angles are identical in the southern and eastern conformations, and the mean values for this angle in the annealed structures of the two conformations differ by only 1°. There are also no notable differences in the Co−A15 and Co−NB3 bond lengths between the southern and eastern conformations. The bond length and bond angle values obtained for Ado(Im)Cbl are also quite similar to the data obtained for the modeling of AdoCbl,[32a] although the Co−NB3 bond length in Ado(Im)Cbl is calculated to be approximately 0.02 Å shorter than that in AdoCbl.

The flexibility of the corrin ring can be explored by monitoring the corrin ring fold angle.[12] The consensus and average annealed structures of Ado(Im)Cbl have smaller fold angles than the corresponding AdoCbl structures (Table 1) and also shorter Co−NB3 bond lengths, as is also the case for the comparison of the crystal structures of CN(Im)Cbl and CH_3(Im)Cbl to those of CNCbl and CH_3Cbl.[18] Differences in the consensus and annealed fold angles for the southern and eastern conformations are minor, although greater ranges of fold angles were observed in the annealed structures of the eastern conformation.

Ado(Im)Cbl Thermolysis. (a) Kinetics. The kinetics of Ado(Im)Cbl thermolysis were studied spectrophotometrically[30] in phosphate buffered (pH 7.0) aqueous solution containing a 50-fold excess of the radical trap, H-TEMPO. Rate constants (k_{obs}) were measured at 8 temperatures between 90 and 125 °C (Table 2). To extend the temperature range to lower temperatures (the half-time at 90 °C was 7.6 h), a radiometric method using [A2-^{3}H]Ado(Im)Cbl,

(33) (a) Brown, K. L.; Cheng, S.; Marques, H. M. *Polyhedron* **1998**, *17*, 2213. (b) Marques, H. M.; Hicks, R. P.; Brown, K. L. *Chem. Commun*. **1996**, 1427.

(34) Brown, K. L.; Cheng, S.; Zou, X.; Zubkowski, J. D.; Valente, E. J.; Knapton, L.; Marques, H. M. *Inorg. Chem*. **1997**, *36*, 3666.

Scheme 2

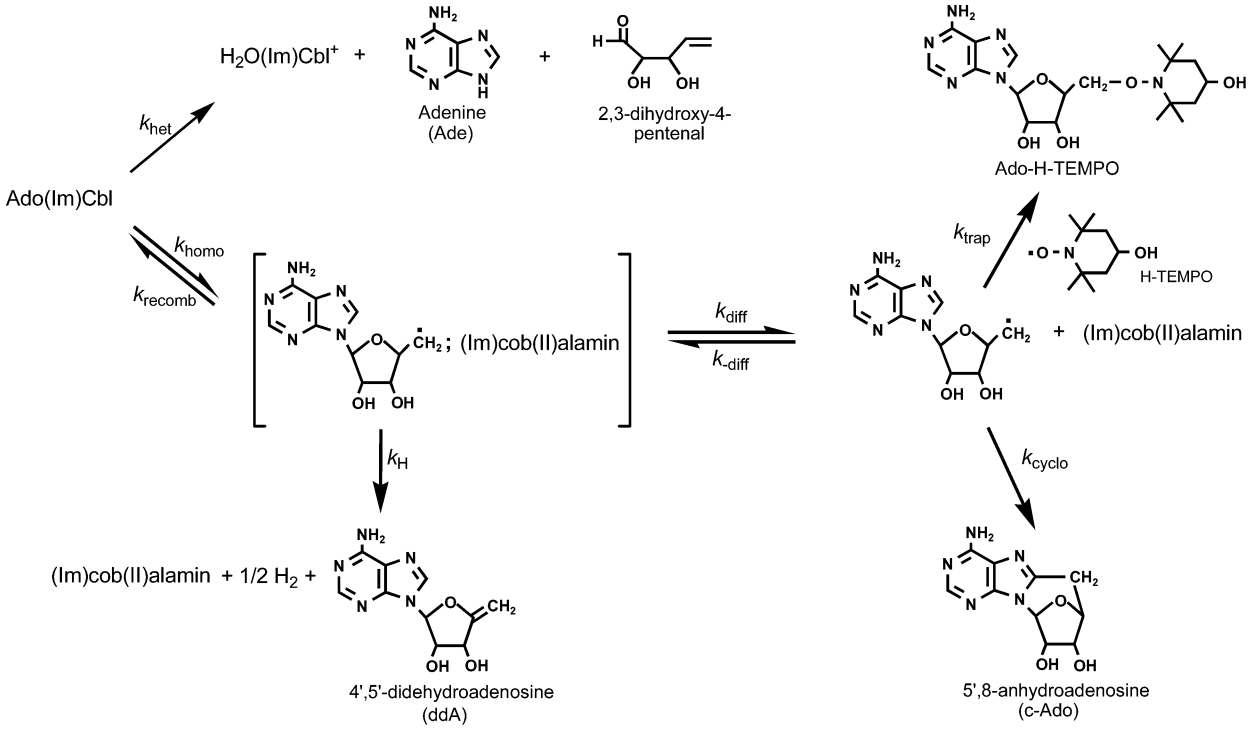

Table 2. Observed Rate Constants and Product Ratios for the Thermolysis of Ado(Im)Cbl

T, °C	k_{obs},[a] s^{-1}	ratio[b]
50.0	$(6.14 \pm 0.16) \times 10^{-7}$ [c]	
70.0	$(3.76 \pm 0.16) \times 10^{-6}$ [c]	0.125 ± 0.002
85.0		0.365 ± 0.005
90.0	$(2.52 \pm 0.30) \times 10^{-5}$	
95.0	$(4.14 \pm 0.11) \times 10^{-5}$	0.670 ± 0.006
100.0	$(6.41 \pm 0.76) \times 10^{-5}$	
105.0	$(1.04 \pm 0.20) \times 10^{-4}$	1.04 ± 0.02
	$(9.53 \pm 0.54) \times 10^{-5}$ [c]	
110.0	$(1.79 \pm 0.06) \times 10^{-4}$	
115.0	$(2.72 \pm 0.21) \times 10^{-4}$	1.92 ± 0.05
120.7	$(4.17 \pm 0.34) \times 10^{-4}$	
125.0	$(5.92 \pm 0.19) \times 10^{-4}$	3.1 ± 0.1

[a] Spectrophotometric method unless otherwise noted. [b] Ratio = [Ado-H-Tempo]/[adenine] = $k_{homo,obs}/k_{het,obs}$. [c] Radiometric method.

as previously described for the thermolysis kinetics of AdoCbl,[2] was employed. Rate constants were measured using the initial rate method[2] at 70 and 50 °C, and a determination at 105 °C (following the reaction for several half-times) agreed well with the spectrophotometric determination at the same temperature (Table 2). At 100 °C, the observed rate constant for Ado(Im)Cbl thermolysis was quite close to that previously observed for AdoCbl.[2,36] An Eyring plot[37] (Figure S1, Supporting Information) was linear and gave the observed activation parameters $\Delta H^{\ddagger}_{obs} = 22.6 \pm 0.1$ kcal mol^{-1} and $\Delta S^{\ddagger}_{obs} = -17.3 \pm 0.3$ cal mol^{-1} K^{-1}.

(b) Product Ratios. The thermal decomposition of 5′-deoxyadenosylcobamides has been well studied.[2,30,36,38] These species decompose via two competing pathways. One involves homolytic dissociation of the Co−C bond,[36,38a−d] a diffusion-controlled reaction which leads to a solvent-caged Co(II)−5′-deoxyadenosyl (Ado•) radical pair.[39] In addition, as is the case for all organocobalt species with β oxygen substituents,[40] 5′-deoxyadenosylcobamides undergo specific acid- and general acid- or solvent-catalyzed heterolysis, in this case to yield an aquacobalt(III) species, adenine (Ade), and 2,3-dihydroxy-4-pentenal (Scheme 2).[36,38a−h,k,m,n] Scheme 2 shows all of the products that can be obtained in aqueous solution. In addition to Ade, several adenine-containing

(35) (a) Lenhert, R. G. *Proc. R. Soc. London A* **1968**, *303*, 45. (b) Bouquiere, J. P.; Finney, J. L.; Lehmann, M. S.; Lindley, P. F.; Savage, H. F. J. *Acta Crystallogr*. **1993**, *B49*, 79.
(36) Hay, B. P.; Finke, R. G. *J. Am. Chem. Soc*. **1986**, *108*, 4820.
(37) (a) Eyring, H. *J. Chem. Phys.* **1935**, *3*, 107. (b) Eyring, H. *Chem. Rev*. **1935**, *18*, 82.
(38) (a) Hay, B. P.; Finke, R. G.; *J. Am. Chem. Soc*. **1987**, *109*, 8012. (b) Hay, B. P.; Finke, R. G. *Polyhedron* **1988**, *7*, 1469. (c) Garr, C. D.; Finke, R. G. *J. Am. Chem. Soc*. **1992**, *114*, 10440. (d) Garr, C. D.; Finke, C. D. *Inorg. Chem*. **1993**, *32*, 4414. (e) Garr, C. D.; Sirovatka, J. M.; Finke, R. G. *J. Am. Chem. Soc*. **1996**, *118*, 11142. (f) Sirovatke, J. M.; Finke, R. G. *J. Am. Chem. Soc*. **1997**, *119*, 3057. (g) Flemming, P. E.; Daikh, B. E.; Finke, R. G. *J. Inorg. Biochem*. **1998**, *69*, 45. (h) Sirovatka, J. M.; Finke, R. G. *Inorg. Chem*. **1999**, *38*, 1967. (i) Gerards, L. E. H.; Bulthuis, H.; deBolster, M. W. G.; Balt, S. *Inorg. Chim. Acta* **1991**, *190*, 47. (j) Gamelkoorn, H. J.; deBolster, M. W. G.; Balt, S. *Recl. Trav. Chim. Pays-Bas* **1992**, *111*, 178. (k) Gerards, L. E. H.; Balt, S. *Recl. Trav. Chim. Pays-Bas* **1992**, *111*, 411. (l) Gerards, L. E. H.; deBolster, M. W. G.; Balt, S. *Inorg. Chim. Acta* **1992**, *192*, 287. (m) Gerards, L. E. H.; Balt, S. *Recl. Trav. Chim. Pays-Bas* **1994**, *113*, 137. (n) Hogenkamp, H. P. C.; Oikawa, T. G. *J. Biol. Chem*. **1964**, *239*, 1911.
(39) (a) Koenig, T.; Finke, R. G. *J. Am. Chem. Soc*. **1988**, *110*, 2657. (b) Keonig, T. W.; Hay, B. P.; Finke, R. G. *Polyhedron* **1988**, *7*, 1499.
(40) (a) Schrauzer, G. N.; Windgassen, R. J. *J. Am. Chem. Soc*. **1967**, *89*, 143. (b) Schrauzer, G. N.; Sibert, J. W. *J. Am. Chem. Soc*. **1970**, *92* 1022. (c) Parfenov, E. A.; Chervykova, T. G.; Edelev, M. G.; Shmyrev, I. K.; Yurkevich, A. M. *Zh. Obshch. Khim*. **1974**, *44*, 1813. (d) Brown, K. L.; Ingrahm, L. L. *J. Am. Chem. Soc*. **1974**, *96*, 7691. (e) Brown, K. L.; Salmon, L.; Kirby, J. A. *Organometallics* **1992**, *11*, 422. (f) Espenson, J. H.; Wang, D. M. *Inorg. Chem*. **1979**, *18*, 2857. (g) Golding, B. M.; Holland, H. L.; Horn, U.; Sakrikar, S. *Angew. Chem., Int. Ed. Engl*. **1970**, *9*, 959. (h) Curzon, E. H.; Golding, B. M.; Wong, Y. *J. Chem. Soc., Chem. Commun.* **1982**, *63*. (i)Vickery, T. M.; Wight, E. E.; Kok, R. A. *Inorg. Nucl. Chem*. **1979**, *15*, 317. (j) Silverman, R. B.; Dolphin, D. *J. Am. Chem. Soc*. **1972**, *94*, 4028. (k) Silverman, R. B.; Dolphin, D. *J. Am. Chem. Soc*. **1975**, *97*, 2924.

products can be obtained from the caged radical pair that results from Co−C bond homolysis. These include 4′,5′-didehydroadenosine (ddA), from an in-cage electron-transfer process,[38c] 5′,8-anhydroadenosine (c-Ado) from the cyclization of the Ado• free radical,[36,41] and, in the presence of the radical trap, H-TEMPO, the trapped Ado• radical, Ado-H-TEMPO. Under the conditions of the current experiments (a 50-fold molar excess of H-TEMPO), the only products detected from the thermolysis of Ado(Im)Cbl were Ade and Ado-H-TEMPO. These observations demonstrate that the solvent cage is not sufficiently robust to allow the in-cage electron-transfer process to occur[38c] and that the trapping conditions are competent to completely suppress the cyclization of the Ado• free radical.

The ratio of [Ado-H-TEMPO]/[Ade] was determined by HPLC analysis at six temperatures between 70 and 125 °C (Table 2). These ratios are strikingly different from those previously observed for the thermolysis of AdoCbl.[2,36] For example, at 100 °C, thermolysis of Ado(Im)Cbl occurs via 47% homolysis and 53% heterolysis, but for AdoCbl, the partitioning at this temperature is 96% homolysis and 4% heterolysis.[2,36]

Since the ratio of the products for parallel first-order processes is equal to the ratio of the rate constants (eq 2), a plot of ln(ratio) vs $1/T$ was linear (Figure S2, Supporting Information).[42] In addition, for parallel first-order processes, the observed rate constant is the sum of the rate constants for the two processes (eq 3). Equations 2 and 3 permit deconvolution of the observed rate constants into the rate constants for the two processes (Table S2, Supporting Information). Eyring plots for $k_{homo,obs}$ and $k_{het,obs}$ (Figure S3, Supporting Information) were satisfactorily linear and gave the values $\Delta H^{\ddagger}_{homo,obs} = 34.1 \pm 0.2$ kcal mol^{-1} and $\Delta S^{\ddagger}_{homo,obs} = 11.5 \pm 0.5$ cal mol^{-1} K^{-1} for homolysis and $\Delta H^{\ddagger}_{het,obs} = 18.1 \pm 0.2$ kcal mol^{-1} and $\Delta S^{\ddagger}_{homo,obs} = -31.1 \pm 0.5$ cal mol^{-1} K^{-1} for heterolysis.

$$[\text{Ado-H-TEMPO}]/[\text{Ade}] = k_{homo,obs}/k_{het,obs} \quad (2)$$

$$k_{obs} = k_{homo,obs} + k_{het,obs} \quad (3)$$

(c) Correction for the Base-On/Base-Off Equilibrium. All cobalamins are known to undergo dissociation and protonation of the axial base in sufficiently acidic media (i.e., the reverse of eq 1.)[43] Equation 1 can be seen to be a composite of the consequtive equilibria shown in eqs 4 and 5.[44]

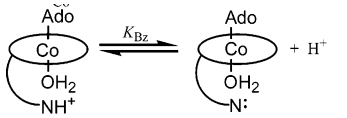

(4)

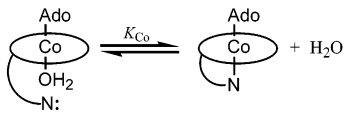

(5)

(41) (a) Hogenkamp, H. P. C. *J. Biol. Chem.* **1963**, *238*, 477. (b) Duong, K. N. V.; Gaudemer, A.; Johnson, M. D.; Quillivic, R.; Zyber, J. *Tetrahedron Lett.* **1975**, *34*, 2997.

Table 3. Acid−Base Chemistry of Ado(Im)Cbl and 1-α-D-Ribofuranosylimidazole

T, °C	p$K_{base-off}$[a]	pK_a[b]
10.0	5.42 ± 0.02	
10.7		6.83 ± 0.02
20.0	5.33 ± 0.02	
19.7		6.77 ± 0.02
30.4		6.45 ± 0.01
31.0	5.21 ± 0.01	
40.0	5.12 ± 0.01	
40.5		6.24 ± 0.01
49.0	5.02 ± 0.02	
49.5		6.09 ± 0.02

[a] Equation 1. Ado(Im)Cbl was titrated spectrophotometrically. [b] For the conjugate acid of 1-α-D-ribofuranosylimidazole, determined potentiometrically. These values are taken as values of pK_{Bz} (eq 4) for the purpose of calculating K_{Co} for Ado(Im)Cbl via eq 6.

From these equilibria, eq 6 may be derived, which relates $K_{base-off}$ (eq 1) to K_{Bz} (eq 4), the K_a of the conjugate acid of the uncoordinated axial nucleoside, and K_{Co} (eq 5), the equilibrium constant for the ligand exchange in which the base-on species is formed. Equation 6 permits the calculation of K_{Co} from the measurable quantities pK base-off and pK_{Bz}.

$$K_{base-off} = (1 + K_{Co})K_{Bz} \quad (6)$$

For alkylCbl's, K_{Co} may be small enough for significant amounts of the base-off species to exist in neutral solution. In addition, since eq 5 is invariably exothermic,[44] K_{Co} decreases with increasing temperature and so the proportion of base-off species is greater at higher temperatures. As a result, the observed rate constants for homolysis and heterolysis are composites of the intrinsic rate constants for the base-on and base-off species, as seen in eqs 7 and 8, where α_{on} is the fraction of base-on species ($\alpha_{on} = K_{Co}/(K_{Co} + 1)$).

$$k_{homo,obs} = \alpha_{on}k_{homo,on} + (1 - \alpha_{on})k_{homo,off} \quad (7)$$

$$k_{het,obs} = \alpha_{on}k_{het,on} + (1 - \alpha_{on})k_{het,off} \quad (8)$$

To calculate values of K_{Co} from eq 6, p$K_{base-off}$ was determined spectrophotometrically at five temperatures between 10 and 49 °C. Values of pK_{Bz} were taken to be equivalent to the pK_a of the conjugate acid of the detached axial nucleoside,[31,45] 1-α-D-ribofuranosylimidazole, which was titrated potentiometrically at five temperatures between 10 and 50 °C. The values are listed in Table 3. The value of p$K_{base-off}$ for Ado(Im)Cbl at 25 °C (5.26) is about 1.6 units higher than that for AdoCbl (3.67[46]), while the detached axial nucleoside, 1-α-D-ribofuranosylimidazole (pK_a = 6.54 at 25 °C), is about 1 order of magnitude more basic than the detached axial nucleoside from AdoCbl, 1-α-D-ribofuranosyl-

(42) From transition state theory,[37] $\ln(k_{homo,obs}/k_{het,obs}) = [(\Delta S^{\ddagger}_{homo,obs} - \Delta S^{\ddagger}_{het,obs})/R] - [(\Delta H^{\ddagger}_{homo,obs} - \Delta H^{\ddagger}_{het,obs})/RT]$.

(43) Ladd, J. N.; Hogenkamp, H. P. C.; Barker, H. A. *J. Biol. Chem.* **1961**, *236*, 2114.

(44) Brown, K. L.; Peck-Siler, S. *Inorg. Chem.* **1988**, *27*, 3548.

(45) (a) For the naturally occurring axial nucleoside, 1-α-D-ribofuranosyl-5,6-dimethylbenzimidazole (α-ribazole), the pK_a of the conjugate acid of the detached nucleoside is essentially identical with that of the zwitterionic form of the detached nucleotide.[45b] (b) Brown, K. L. *J. Am. Chem. Soc.* **1987**, *109*, 2277.

(46) Brown, K. L.; Hakimi, J. M.; Jacobsen, D. W. *J. Am. Chem. Soc.* **1984**, *106*, 7894.

Table 4. Comparison of the Acid−Base Chemistry and K_{Co} for Ado(Im)Cbl and AdoCbl

	Ado(Im)Cbl	AdoCbl
$pK_{base-off}$		
value at 25 °C	5.26[a]	3.67[b]
pK_{Bz}		
value at 25 °C	6.54[a]	5.56[c]
$\Delta H°_{Bz}$, kcal mol^{-1}	8.1 ± 0.2[d]	6.4 ± 0.4[c]
$\Delta S°_{Bz}$, cal mol^{-1} K^{-1}	−2.8 ± 0.7[d]	−4.1 ± 1.5[c]
K_{Co}		
value at 25 °C	18.0[e]	76.6[c]
$\Delta H°_{Co}$, kcal mol^{-1}	−4.3 ± 0.2[f]	−5.6 ± 0.9[g]
$\Delta S°_{Co}$, cal mol^{-1} K^{-1}	−8.6 ± 0.5[f]	−13 ± 3[g]

[a] Interpolated from the data in Table 3. [b] Reference 46. [c] Reference 31. [d] From a plot (not shown) of ln K_{Bz} (pK_a in Table 3) vs 1/T. [e] Interpolated from values calculated from the data in Table 3 via eq 6. [f] From a plot (not shown) of ln K_{Co} (calculated via eq 6 from the values in Table 3) vs 1/T. [g] Reference 36.

5,6-dimethylbenzimidazole (α-ribazole, pK_a = 5.56 at 25 °C[31]). Table 4 provides a comparison of the acid−base chemistry of Ado(Im)Cbl and AdoCbl and their axial nucleosides.

For all organocobalamin Co−C bond homolyses which have been studied, the base-off species is much less reactive than the base-on species (sometimes referred to as the base-on effect),[10a,b,38a,47] so that $k_{homo,on}$ can be calculated as $k_{homo,obs}/\alpha_{on}$ (i.e., omitting the $k_{homo,off}$ term in eq 7).[48] It is similarly clear that the heterolytic reactivity of the carbon−cobalt bond on base-off AdoCbl is much lower than that of the base-on species,[38a,40e,49] so that $k_{het,on}$ may be calculated as $k_{het,obs}/\alpha_{on}$.[50] The calculated values of $k_{homo,on}$, $k_{het,on}$, and K_{Co} are given in Table S3 (Supporting Information). Eyring plots (Figure 4) of $k_{homo,on}$ and $k_{het,on}$ were satisfactorily linear and led to the activation parameters for homolysis and heterolysis listed in Table 5, along with those previously determined for AdoCbl.[2] As was the case for AdoCbl[2], homolysis is faster than heterolysis at high temperatures, but heterolysis is faster at low temperatures, the isokinetic point being 102.4°. At 100 °C, homolysis of Ado(Im)Cbl is 3.3-fold slower than for AdoCbl, and at 37 °C, Ado(Im)Cbl homolysis is 4.3-fold slower than that for AdoCbl. This is the result of a 1.0 ± 0.4 kcal mol^{-1} increase in the enthalpy of activation for homolysis of Ado(Im)Cbl relative to AdoCbl. The entropies of activation, in contrast, are identical. The situation for heterolysis is the reverse. Ado(Im)Cbl heterolysis is about 8.5-fold faster than AdoCbl heterolysis, regardless of the temperature, the result of identical enthalpies of activation, but an entropy of activation for Ado(Im)Cbl that is 4.9 ± 1.1 cal mol^{-1} K^{-1} less negative than that for AdoCbl.

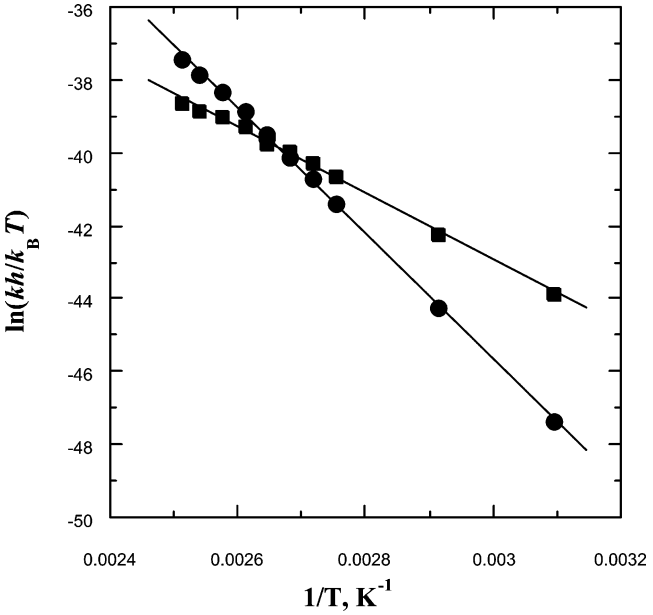

Figure 4. Eyring plots for the homolysis ($k_{homo,on}$, ●) and heterolysis ($k_{het,on}$, ■) of Ado(Im)Cbl. The solid lines are linear regressions: $k_{homo,on}$, slope = −17,495 ± 166 K, intercept = 6.914 ± 0.448, r^2 = 0.999; $k_{het,on}$, slope = −9,390 ± 165 K, intercept = −14.67 ± 0.45, r^2 = 0.997.

Table 5. Comparison of the Intrinsic Rate Constants and Activation Parameters for Homolysis and Heterolysis of Ado(Im)Cbl and AdoCbl

	Ado(Im)Cbl	AdoCbl[a]
$k_{homo,on}$		
value at 100 °C, s^{-1}	3.40 × 10^{-5}	1.12 × 10^{-4}
value at 37 °C, s^{-1}	2.07 × 10^{-9}	8.88 × 10^{-9}
$\Delta H_{homo,on}$, kcal mol^{-1}	34.8 ± 0.3	33.8 ± 0.2
$\Delta S_{homo,on}$, cal mol^{-1} K^{-1}	13.7 ± 0.9	13.5 ± 0.7
$k_{het,on}$		
value at 100 °C, s^{-1}	3.90 × 10^{-5}	4.46 × 10^{-6}
value at 37 °C, s^{-1}	1.95 × 10^{-7}	2.36 × 10^{-8}
$\Delta H_{het,on}$, kcal mol^{-1}	18.7 ± 0.3	18.5 ± 0.2
$\Delta S_{het,on}$, cal mol^{-1} K^{-1}	−29.1 ± 0.9	−34.0 ± 0.7

[a] Reference 2.

Discussion

In all reported crystal structures of AdoCbl,[11,35,51] the adenyl moiety (Ade) of the Ado ligand is always found to be positioned over the C ring when viewed from the upper or β face of the corrin, referred to as the southern conformation. Similarly, AdoCbl analogues, including (α-ribo)-AdoCbl,[29b] in which the configuration of the N-glycosidic bond in the Ado ligand is inverted, and IsoAdoCbl,[30] in which the upper axial ligand is isoadenosine, all have southern conformations as the global minimum. In solution, however, NMR observations[32a,52] and molecular model-

(47) (a) Brody, J. D. *Proc. Natl. Acad. Sci. U.S.A.* **1969**, *62*, 461. (b) Schrauzer, G. N.; Lee, L. P.; Sibert, J. W. *J. Am. Chem. Soc*. **1970**, *92*, 2997. (c) Chamaly, S. M.; Pratt, J. M. *J. Chem. Soc., Dalton Trans*. **1980**, 2259. (d) Chamaly, S. M.; Pratt, J. M. *J. Chem. Soc., Dalton Trans.* **1980**, 2274. (e) Blau, R. J.; Espenson, J. H. *J. Am. Chem. Soc*. **1985**, *107*, 3530. (f) Brown, K. L.; Brooks, H. B. *Inorg. Chem.* **1991**, *30*, 3421. (g) Waddington, M. D.; Finke, R. G. *J. Am. Chem. Soc*. **1993**, *115*, 4629. (h) Brown, K. L.; Cheng, S.; Marques, H. M. *Inorg. Chem.* **1995**, *34*, 3038.

(48) The assumption can be tested using the thermolysis data for the axial base-free analogue of AdoCbl, AdoCbi$^+$ of Hay and Finke,[38a] assuming that AdoCbi$^+$ is an accurate model for the reactivity of the base-off species of Ado(Im)Cbl. For example, using the value of k_{homo} for AdoCbi$^+$ at 100 °C (2.63 × 10^{-6} s^{-1}) as $k_{homo,off}$ in eq 7, gives a value of 3.53 × 10^{-5} s^{-1} for $k_{homo,on}$, while omitting the $k_{homo,off}$ term entirely gives a value of $k_{homo,on}$ of 3.58 × 10^{-5} s^{-1}, a difference of 1.4%, well within experimental error.

(49) Jensen, M. P. Halpern, J. *J. Am. Chem. Soc*. **1999**, *121*, 2181.

(50) This assumption can similarly[48] be tested using the Hay and Finke data[38a] for AdoCbi$^+$. Thus, using the value of k_{het} for AdoCbi$^+$ at 100 °C (2.07 × 10^{-7} s^{-1}) as $k_{het,on}$ in eq 8, gives 4.10 × 10^{-5} s^{-1} for $k_{het,on}$, while ignoring the second term in eq 8 gives the identical value (to three significant figures).

(51) (a) Savage, H. *Biophys. J*. **1989**, *50*, 947. (b) Bouquiere, J. P.; Finney, J. L.; Savage, H. F. J. *Acta Crystallogr., Sect. B* **1994**, *50*, 566.

ing[26a,32a,b,53] of AdoCbl have confirmed that an eastern conformation (where the Ado ligand is rotated ca. 50° counterclockwise about the Co−A15 bond when viewed from above) is populated at room temperature. Modeling also predicts northern and western conformations (where the Ade is over C5 and the C1−C19 bridge, respectively) which should be accessible in solution, and this was subsequently confirmed by nOe data collected at elevated temperatures.[32a] Ado(Im)Cbl is thus unique in having an eastern conformation as the global minimum, and it is consequently most unfortunate that we have been unable to crystallize this derivative to determine if the unique eastern conformation occurs in the solid state. Conversely, the population of two readily accessible conformations at ordinary temperatures may be responsible for the complex's failure to crystallize.

In the consensus structures of Ado(Im)Cbl, the tilt angle of the α ligand (−1.8° for the southern conformation and −2.1° for the eastern conformation) is smaller than the tilt angle of AdoCbl (Figure 3F, the average tilt angle for AdoCbl is 4.4 ± 0.9°[11,35,51]). Thus, in Ado(Im)Cbl, the axial base tilts slightly toward C5, while, in AdoCbl, it tilts away from C5. In AdoCbl, the hydrogen at position B4 of the Bzm base comes into van der Waals contact with the C4, C5, and C6 region of the corrin ring,[18a] effectively forcing the bulky ligand "downward". No such interaction occurs with the smaller axial base in Ado(Im)Cbl and, hence, the tilt angle is smaller.

The calculated Co−NB3 bond lengths in both conformations of Ado(Im)Cbl (Table 1) are slightly shorter (0.02 Å) than in AdoCbl, undoubtedly a consequence of the reduced size of the α axial base and the consequent reduced tilt angle in Ado(Im)Cbl. Note, however, that we have previously pointed out[32b,53a] that the MM2 cobalamin force field underestimates the length of the Co−NB3 bond since the bond stretching parameter was developed to model the *average* Co−NB3 bond trans to an alkyl ligand. This can be seen in Table 1 by the differences between the length of the Co−NB3 bond in the crystal structures of AdoCbl and in the calculated structures. Thus, the length of the Co−NB3 bond in Ado(Im)Cbl is likely to be underestimated as well, but once this is accounted for, one can still get a "good feel" for how the length of the Co−NB3 bond changes when the Bzm base is replaced by imidazole.

A correlation has been observed between the corrin ring fold angle and the length of the Co−NB3 bond in a variety of XCbl's.[54] This correlation leads to the conclusion that shorter Co−NB3 bonds result in increased steric repulsion between the Bzm base and the lower face of the corrin, which in turn results in larger fold angles.[18a,b,54] However, the opposite trend is observed in the consensus and average annealed structures of Ado(Im)Cbl, which are less folded, and have shorter Co−NB3 bonds, than the corresponding AdoCbl structures (Table 1). Fold angles for the southern conformation of Ado(Im)Cbl are also less than those observed in the crystal structures of AdoCbl. This is undoubtedly due to the smaller steric size of the imidazole axial ligand which allows a closer approach of the base to the corrin with less steric interaction. In earlier MM studies of mechanochemical triggering,[14] shortening of the axial Co−NB3 bond of Ado(Im)Cbl did indeed cause increased upward folding of the corrin ring.

The acid−base chemistry of Ado(Im)Cbl and its axial nucleoside reveal some surprises (Table 4). The value of $pK_{base-off}$ for Ado(Im)Cbl (5.26 at 25 °C) is considerably higher than that for AdoCbl (3.67 at 25 °C), at least in part due to the higher basicity of the α-imidazole nucleoside compared to Bzm. In addition, the value of K_{Co} (eq 5) for Ado(Im)Cbl (18.0 at 25 °C) is smaller than that for AdoCbl (76.6 at 25 °C), despite the fact that the axial nucleoside is more basic than Bzm and is smaller than Bzm, and the Co−NB3 bond is apparently shorter in Ado(Im)Cbl than in AdoCbl. This could be the result of a hydrophobic effect of the "greasy" Bzm ligand. The results imply that the base-on form of AdoCbl is slightly less than 1 kcal mol^{-1} more stable than the base-on form of Ado(Im)Cbl, relative to the base-off species, assuming that the free energies of the base-off forms are the same. However, since the current study represents the first determination of a value for K_{Co} in a cobamide with an axial base other than Bzm, the effect of axial nucleoside basicity on the internal ligation equilibrium is actually unknown. Existing values[10f,38e,f,47a,55,56] of the intermolecular binding constants for exogenous ligands with alkylcobinamides ($RCbi^+$'s, analogues of RCbl's missing the axial nucleotide) do show small increases in binding affinity with increasing ligand basicity, but the individual values are invariably very small (and consequently difficult to measure accurately), as is the range of observed values. Clearly, the effect of basicity on the intramolecular formation of base-on R(X)Cbl's needs further study, and work along these lines is in progress. We also note with interest that the values of $\Delta H°_{Co}$ for both Ado(Im)Cbl and AdoCbl fall well outside the experimental limits of the invariant value of −7.9 ± 0.7 kcal mol^{-1} previously observed for series of 8 RCbl's,[44] suggesting that the Ado ligand has some influence, probably steric, on the axial ligation energetics.[32b,57]

We also note that Sirovatka and Finke[38f] have measured values for the intermolecular binding constant for 1-methylimidazole to $AdoCbi^+$ (0.5 M^{-1}) along with thermodynamic values (ΔH = −7.8 ± 0.4 kcal mol^{-1} and ΔS = −28 ± 1 cal mol^{-1} K^{-1}), albeit in ethylene glycol rather than in water. These permit, for the first time, an estimate of the intramolecular advantage of tethering the axial nucleoside to the molecule, which amounts to an apparent

(52) Bax, A.; Marzilli, L. G.; Summers, M. F. *J. Am. Chem. Soc*. **1987**, *109*, 566.
(53) (a) Marques, H. M.; Brown, K. L. *Inorg. Chem*. **1995**, *34*, 3733. (b) Marques, H. M.; Ngoma, B.; Egan, T. J.; Brown, K. L. *J. Mol. Struct*. **2001**, *561*, 71.
(54) Kratky, C.; Fäber, G.; Gruber, K.; Wilson, K.; Dauter, Z.; Nolting, H.; Konrat, R.; Kräutler, B. *J. Am. Chem. Soc*. **1995**, *117*, 4654.
(55) (a) Pailes, W. H.; Hogenkamp, H. P. C. *Biochemistry* **1968**, *7*, 4160. (b) Baldwin, D. A.; Betterton, E. A.; Chemaly, S. M.; Pratt, J. M. *J. Chem. Soc., Dalton Trans*. **1985**, 1613. (c) Brown, K. L.; Satyanarayana, S. *Inorg. Chim. Acta* **1992**, *201*, 113.
(56) Garr, C. D.; Sirovatka, J. M.; Finke, R. G. *Inorg. Chem*. **1996**, *35*, 5912.
(57) Calafat, A. M.; Marzilli, L. G. *J. Am. Chem. Soc*. **1993**, *115*, 9182.

Scheme 3

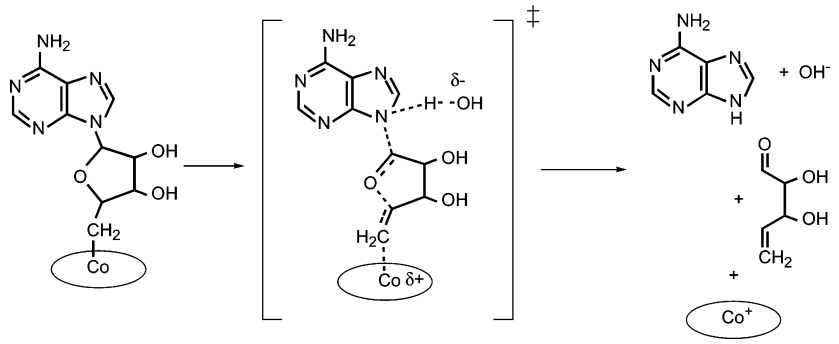

ligand concentration of 36 M. The effect, as anticipated, is largely an entropic one.

The current results show that, at 100 °C, thermolysis of Ado(Im)Cbl proceeds with 54% heterolysis, compared to 4% heterolysis for AdoCbl at the same temperature.[2,36] This result is nearly identical with that previously found by Sirovatka and Finke[58] for the thermolysis of Ado(N-MeIm)Cbi$^+$, generated in situ by addition of exogenous *N*-methylimidazole (N-MeIm) to AdoCbi$^+$. The striking difference in outcome for Ado(Im)Cbl and AdoCbl is seen here to be the result of a 3-fold decrease in the rate constant for homolysis of Ado(Im)Cbl coupled with a 9.4-fold increase in the rate constant for heterolysis. In a recent reexamination[59] of the earlier work[38e,f,56,58] in this area, Doll and Finke concluded that the increased heterolysis in Ado(N-MeIm)Cbi$^+$ was due to the formation and subsequent ligation to AdoCbi$^+$ of the solvent anion (in this case, ethylene glycolate) which is formed in significant quantities in these experiments due to the very low binding constant of *N*-MeIm and the consequent need to employ it in large excess. This, however, cannot be the case for Ado(Im)Cbl since the axial imidazole ligand is tethered to the cobamide and consequently employed in small molar amounts and the reaction solutions are buffered. Instead, we attribute the reduction in the homolysis rate constant to the reduced fold angle in Ado(Im)Cbl, consistent with the molecular modeling of mechanochemical triggering[14] which shows that the smaller Im axial base and accompanying reduced corrin ring fold angle put less steric strain on the Co−C bond than occurs in AdoCbl. While there is a significant difference in basicity between the Im and Bzm axial nucleosides, axial ligand basicity is not expected to significantly affect Co−C bond homolysis as the reaction proceeds without the generation of any charge separation. Conversely, we attribute the increase in heterolysis rate constant for Ado(Im)Cbl to the increased basicity of the axial nucleoside. In this case (Scheme 3) the reaction does produce a separation of charge, and the emerging positive charge on the cobalt atom should be stabilized by increased basicity of the axial ligand. Finke's earlier work[38e] on the effect of exogenous substituted pyridine bases on the thermolysis of AdoCbi$^+$ suggests that this is the case, with the rate constant for Ado(X-py)Cbi$^+$ heterolysis increasing by 17-fold when the substituted pyridine ligand is changed from py (pK_a = 6) to 4-Me$_2$N-py (pK_a = 9.2). Clearly, additional work on the effect of axial nucleoside basicity on Co−C bond homolysis and heterolysis is needed.

Table 6. Comparison of the Enzymatic and Nonenzymatic Co−C Bond Homolysis of Ado(Im)Cbl and AdoCbl with Ribonucleoside Triphosphate Reductase (RTPR) at 37 °C

	Ado(Im)Cbl	AdoCbl[a]
$k_{homo,on}$, s^{-1}	2.1×10^{-9}	8.9×10^{-9}
k_{enz}, s^{-1} [b]	0.83[c]	13.7
catal efficiency[d]	4.0×10^{8}	1.5×10^{9}
$\Delta G_{enz} - \Delta G_{homo,on}$, kcal mol^{-1}	12.2	13.0
K_{eq}^{nonenz} [e]	1.9×10^{-18}	7.9×10^{-18}
K_{eq}^{enz} [f]	4.6×10^{-6}	2.3×10^{-5}
$K_{eq}^{enz}/K_{eq}^{nonenz}$	2.4×10^{12}	3.0×10^{12}
$\Delta G°_{enz} - \Delta G°_{nonenz}$, kcal mol^{-1}	17.6	17.7

[a] References 1 and 16. [b] The forward rate constant for RTPR-induced Co−C bond homolysis at 37 °C (k_f in refs 1 and 16). [c] Reference 16. [d] Calculate as $k_{enz}/k_{homo,on}$. [e] The equilibrium constant for nonenzymatic thermal homolysis. See text. [f] Calculated from the measured equilibrium constant for formation of cob(II)alamin at the enzyme active site, as described in ref 2.

At 37 °C, the homolysis of Ado(Im)Cbl is 4.3-fold (0.9 kcal mol^{-1}) slower than that of AdoCbl (Table 5). This is consistent with the smaller corrin ring fold angle for Ado(Im)Cbl (Table 1) and molecular modeling studies[14] which show a reduced fold angle in Ado(Im)Cbl is accompanied by a reduction in the steric strain placed on the Co−C bond by the upwardly folded corrin. The availability of the rate constant for Ado(Im)Cbl homolysis permits calculation of the equilibrium constant for homolysis, assuming that the reverse process, the recombination of (Im)cob(II)alamin and the Ado$^\bullet$ radical, is diffusion controlled and has the same rate constant as the recombination of cob(II)alamin and Ado$^\bullet$ ($(1.1 \pm 0.2) \times 10^9$ s^{-1}).[2,60] The value obtained (1.9×10^{-18}, Table 6) is, of course, 4.3-fold smaller than that for AdoCbl.[2]

The rate and equilibrium constants for enzyme-induced homolysis of Ado(Im)Cbl with the AdoCbl-dependent RTPR[16] can now be compared to the current nonenzymatic values (Table 6). While the enzyme-induced homolysis of Ado(Im)Cbl is 16-fold slower than that for AdoCbl, the nonenzymatic homolysis is 4.3-fold slower. The net result is that the catalytic efficiency of the enzyme for the homolysis of the Co−C bond of Ado(Im)Cbl (4×10^8, 12.2 kcal mol^{-1}) is 3.8-lower than for AdoCbl, a difference

(58) Sirovatka, J. M.; Finke, R. G. *Inorg. Chem.* **1999**, *38*, 1697.
(59) Doll, K. M.; Finke, R. G. *Inorg. Chem.* **2004**, *43*, 2611.
(60) (a) Endicott, J. F.; Netzel, T. L. *J. Am. Chem. Soc.* **1979**, *101*, 4000. (b) Chagovitz, A. M.; Grisson, C. B. *J. Am. Chem. Soc.* **1993**, *115*, 12152. (b) Waker, L. A.; Shiang, J. J.; Anderson, N. A.; Pullen, S. H.; Sension, R. J. *J. Am. Chem. Soc.* **1998**, *120*, 7286.

of 0.8 kcal mol^{-1}. Given the likelihood that the increased basicity of the axial nucleoside in Ado(Im)Cbl does not significantly affect the homolysis rate (vide supra), we conclude that the steric bulk of the axial Bzm nucleoside contributes less than 1 kcal mol^{-1} to the enzymatic activation of AdoCbl and, consequently, that ground state mechanochemical triggering does not significantly contribute to the 13 kcal mol^{-1} lowering of the activation energy for Co−C bond homolysis of AdoCbl generated by the RTPR enzyme.

As we have pointed out previously,[1,2] in addition to catalyzing the homolysis of AdoCbl by 9 orders of magnitude, RTPR also shifts the equilibrium for homolysis by 12 orders of magnitude toward the radical pair products, as a result of differential binding of the coenzyme and the homolysis products to the enzyme active site. Together with an additional thermodynamic "pull" of about 4 orders of magnitude[1,2] exerted by the favorable transfer of a hydrogen atom from an active site cysteine residue to the product Ado• radical to generate a catalytically essential thiyl radical,[61] the enzyme generates a stoichiometrically significant amount of radical at the active site, despite the use of a bond dissociation which is inherently extremely thermodynamically unfavorable. The equilibrium constant for enzyme-catalyzed Ado(Im)Cbl Co−C bond homolysis may similarly be calculated from the observed value of the equilibrium constant for formation of (Im)cob(II)alamin at the active site,[16] by correcting for the subsequent equilibrium transfer of the cysteine hydrogen to form the thiyl radical. The resulting value (Table 6), 4.6×10^{-6}, is 5-fold smaller than that for AdoCbl itself. As the nonenzymatic equilibrium constant for homolysis of Ado(Im)Cbl is about 4-fold smaller than that for AdoCbl, the net result is that enzyme-induced shift of the equilibrium ($K_{eq}^{enz}/K_{eq}^{nonenz}$, Table 6) is essentially the same for both coenzymes. Hence, the differential binding of coenzyme and homolysis products by the enzyme is not affected by the change in axial nucleoside.

In summary, the present results, together with our earlier measurement[16] of the rate constant for enzyme-catalyzed homolysis of Ado(Im)Cbl, permit a definitive answer to the question of whether the bulkiness of the naturally occurring Bzm axial base of cobalamins is important in the enzymatic activation of AdoCbl for Co−C bond homolysis. The answer, at least for the class II AdoCbl-dependent ribonucleotide reductase, is that it is not.

Acknowledgment. This research was supported by the National Institute of General Medical Sciences, Grant GM 48858 (to K.L.B.), by the National Research Foundation, Pretoria, South Africa, and the University of the Witwatersrand, through the Molecular Sciences Institute (to H.M.M.).

Supporting Information Available: Table of observed nOe's, an Eyring plot for k_{obs}, a plot of the logarithm of the product ratio vs $1/T$, a table of observed rate constants for homolysis and thermolysis, an Eyring plot for $k_{homo,obs}$ and $k_{het,obs}$, and a table of K_{Co}, α_{on}, and homolysis and heterolysis rate constants for the base-on species of Ado(Im)Cbl. This material is available free of charge via the Internet at http://pubs.acs.org.

IC040079Z

(61) Licht, S.; Gerfen, J.; Stubbe, J. *Science* **1996**, *271*, 477.